J. Synchrotron Rad. (1999). **6**, 653–655

EXAFS studies of the chemical state of lead and copper in corrosion products formed on the brass surface in potable water

Anatoly I. Frenkel[a]*† and Gregory V. Korshin[b]

[a]*Materials Research Laboratory, University of Illinois at Urbana-Champaign, Urbana, IL 61801, USA,* [b]*Department of Civil Engineering, University of Washington, Seattle, WA 98195, USA.* *Email:frenkel@bnl.gov*

Corrosion products formed on the surface of lead-containing brass were examined using grazing incidence fluorescence EXAFS. The corrosion scales were shown to be comprised by malachite $Cu_2(OH)_2CO_3$ and hydrocerussite $Pb_3(OH)_2(CO_3)_2$. The equatorial and axial Cu-O distances in the corrosion deposits were virtually the same as in the reference malachite sample, whereas the disorder in the Cu-O distances in the corrosion products was enhanced. The chemical environment around the Pb atoms in the corrosion deposits was similar to that in hydrocerussite but there was an apparent shortening of the Pb-O nearest neighbor distances in the corrosion deposits compared to those in pure hydrocerussite.

Keywords: brass, corrosion, surface properties, EXAFS

1. Introduction

Lead in potable water constitutes a significant threat to exposed populations. To predict its release, the nature of lead compounds formed because of the corrosion of lead-tin solder and leaded brasses must be known [Schock, 1996; Schock, 1980; Shoesmith, 1988]. In the latter case, lead compounds are often amorphous and mixed with dissimilar species of other metals. Their identification via conventional techniques is difficult. In this work, the brass corrosion products were examined using SEM and grazing incidence fluorescence EXAFS. EXAFS measurements showed that the corrosion scales were comprised by malachite $Cu_2(OH)_2CO_3$ and hydrocerussite $Pb_3(OH)_2(CO_3)_2$.

2. Experiment

The samples (brass faucets) were obtained from a potable water distribution system nearby Seattle, WA for which lead problems had been documented. A thin layer of corrosion deposits was found on the surfaces exposed to potable water. SEM examination showed that the structure of the surface layer was completely amorphous. Structural identification of the surface compounds, therefore, was not possible based on the crystallographic data. It was decided to use EXAFS to probe the nature of the surface compounds.

EXAFS measurements in the corrosion deposits were performed on Bell Labs-UIUC beamline X16C at the NSLS at Brookhaven National Laboratory in grazing incidence fluorescence mode at room temperature. EXAFS in the reference Cu and Pb metal foils, malachite, cerussite and hydrocerussite were measured in transmission. Sagittally focused second crystal in the double crystal Si (111) monochromator allowed to horizontally focus the beam to the 1 mm size at the sample position. Harmonics were rejected by detuning the monochromator (Si 111) by ~ 20%. Lytle detector was used for fluorescence detection. Ni and Ge filters (3 absorption lengths thick each) were used for Cu K edge and Pb L3 edge XAFS measurements, respectively.

Care was taken to ensure that the XAFS signal from corrosion layer only contributes to the total signal. For that, the sample was rotated and XAFS was measured several times and signals were compared until the contribution from the bulk brass vanished.

3. Data analysis and results

EXAFS signals measured at Cu K and Pb L_3 edges in corrosion layer are dramatically different from the respective signals measured in bulk brass and are very similar to those in Cu and Pb metal foils as expected. This difference between the surface layer and bulk signals for Cu K edge data is illustrated in Figs. 1 and 2 in k- and r-spaces, respectively. In particular, the absence of Cu-Cu first nearest neighbors contributions (characterizing the bulk brass signal) to the corrosion layer signal in the r-range between 1.8 and 2.5 Å (Fig. 2) demonstrates that only the local atomic environment around Cu atoms in the corrosion layer contributes to its EXAFS signal. Hence, the Cu K edge and Pb L_3 edge corrosion layer data can be directly compared against the model compounds and theoretical simulations.

Figure 1
Cu K edge k^2-weighted $\chi(k)$ data in the corrosion deposit, bulk brass and malachite.

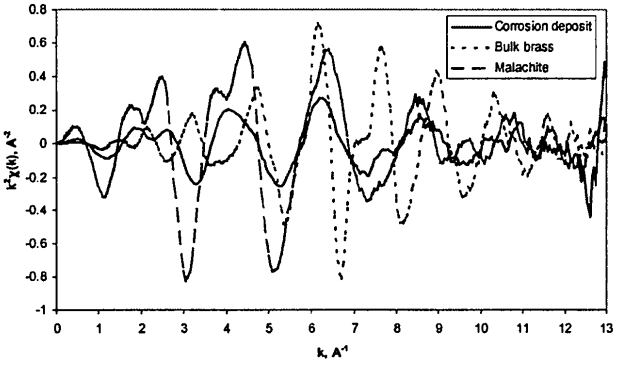

3.1 Cu K edge data.

Malachite $Cu_2(OH)_2CO_3$ is the predominant mineral formed on the copper surface in conditions similar to those at the Mt.Vernon site [Ferguson, 1996; Korshin, 1996]. Since Cu is the major component in the studied alloy (ca. 75 weight %), it was presumed that Cu-containing solids formed on the brass might be similar to those found on pure copper. Therefore, it was decided to use malachite as the reference compound. The data analysis of Cu K edge data was performed by comparing the structure around Cu in the corrosion layer with that in $Cu_2(OH)_2CO_3$. Cu K edge

† Mailing address: Building 510 E, Brookhaven National Laboratory, Upton, NY 11973, USA.

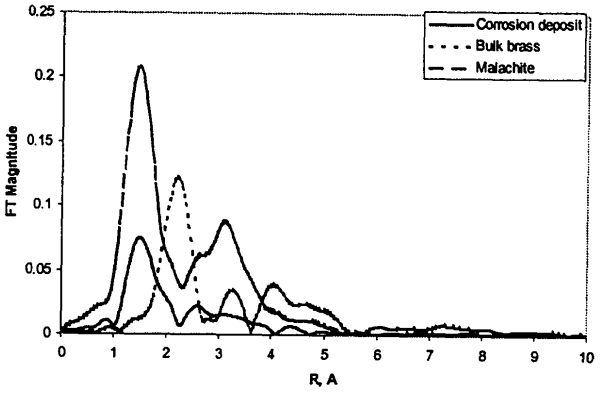

Figure 2
Fourier transform magnitudes of Cu *K* edge k^2-weighted $\chi(k)$ data in the corrosion deposit, bulk brass and malachite.

EXAFS was analyzed using FEFF6 [Zabinsky, 1995] and FEFFIT [Stern, 1995] codes.

Oxygen octahedra constitute the first shell of Cu atoms in malachite. They are split in two subshells with 2 axial oxygens and 4 equatorial oxygens. The distances to these two subshells and their mean square disorders (σ^2) were fitted separately. Another fitting variable was correction to the energy reference, ΔE_0. The data *k*-range was chosen from 3 to 12 $Å^{-1}$ and *r*-range from 1.4 to 2.4 Å which corresponds to the total of 8 independent points. Fit results are summarized in Table 1.

The same model was used to analyze the Cu environment in corrosion layer where the data range was shorter (from 3 to 10 $Å^{-1}$). To decrease the number of fitting variables, the malachite and corrosion layer absorption coefficient data were aligned in energy prior to the background removal and ΔE_0 in fits to the corrosion layer data was fixed at 5 eV as obtained from the fit to malachite. Fit is shown in Fig. 3.

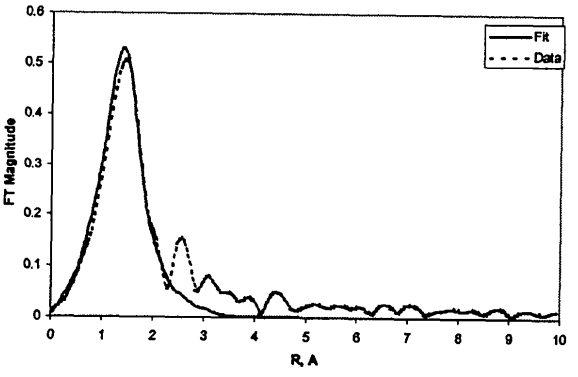

Figure 3
Fourier transform magnitudes of k^2-weighted data and fit of the Cu *K* edge $\chi(k)$ measured in the corrosion deposit.

The Cu-O distances in the corrosion deposits are virtually the same as in reference malachite sample. The disorder in the Cu-O distances in the corrosion products is substantially greater than in malachite (Table 1).

Table 1
Nearest neighbor Cu-O distances and mean square deviations in malachite and the brass surface corrosion deposits.

	R, Å		σ^2, $Å^2$	
	$Cu\text{-}O_{ax}$	$Cu\text{-}O_{eq}$	$Cu\text{-}O_{ax}$	$Cu\text{-}O_{eq}$
Malachite	2.45(1)	1.92(5)	0.017(4)	0.0078(4)
Corrosion deposit	2.48(5)	1.91(1)	0.03(1)	0.017(2)

3.2 *Pb L_3 edge data.*

The literature data indicate that three main types of lead carbonates (cerussite $PbCO_3$, hydrocerussite, plumbonacrite $Pb_{10}(CO_3)_6(OH)_6O$) are predominant solids formed at corroding surfaces in the presence of dissolved carbonates [Schock, 1996; Schock, 1989; Taylor and Lopata, 1984; Colling, 1987; Shoesmith, 1988]. Of those, plumbonacrite is observed only in a narrow range of conditions at pH>13, while hydrocerussite or a mixture of hydrocerussite and cerussite are commonly found. The cerussite and hydrocerussite phases also exhibit interconversion initiated at a fixed pH by a slight depletion of the partial pressure of CO_2 [Taylor and Lopata, 1984]. Calcium and magnesium do not seem to affect the deposits formed on the lead surface. Based on this data, it was decided to select cerussite and hydrocerussite as the main reference materials and compare their EXAFS spectra with those of the corrosion deposits.

Detailed analysis of Pb L_3 edge data using FEFF6 is complicated due to the relatively short available *k*-range (3 to 8 $Å^{-1}$). Qualitatively, the chemical environment of Pb in the corrosion layer was similar to although not identical with that in hydrocerussite (Fig. 4). Since the chemical environment of Pb in another possible model compound, cerussite $PbCO_3$, differed dramatically from that in the corrosion layer, its formation, although often predicted by thermodynamic models [Schock, 1980], was ruled out. Therefore, theoretical evaluation of Pb solubility may be done using hydrocerussite as the dominant lead mineral.

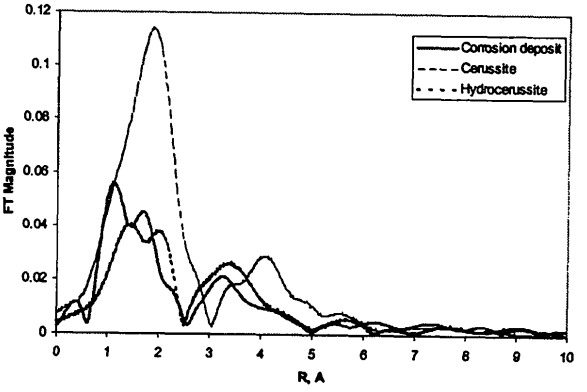

Figure 4
Fourier transform magnitudes of Pb L_3 edge *k*-weighted $\chi(k)$ data in the corrosion deposit, cerussite and hydrocerussite.

Given the positions of the peaks in the Fourier transform magnitudes spectra of the corrosion layer, the Pb-O nearest neighbor bonds in the corrosion products appear to be shortened compared to those in the reference hydrocerussite sample (Fig. 4). Alternatively, this may indicate high anharmonicity of the Pb-O vibrations caused by distortion of the local symmetry in the

hydrocerussite micronuclei dispersed in the matrix of dissimilar corrosion products and/or the presence of mixed Cu-Pb compounds.

4. Conclusions

Malachite and hydrocerussite were found to be the predominant phases formed on the surface of leaded brass corroded in potable water. The Cu-O distances in the corrosion layer are virtually the same as in reference malachite sample but the disorder in the Cu-O distances in the corrosion products is substantially greater than in malachite.

The chemical environment around Pb atoms in corrosion deposits is similar to that in hydrocerussite although the Pb-O nearest neighbor bonds in the corrosion products appear to be shortened compared to those in hydrocerussite. This is likely to indicate high anharmonicity of the Pb-NN vibrations associated with the distortion of the local symmetry in the hydrocerussite micronuclei.

This study seems to constitute the first attempt to explore the nature of copper and lead corrosion products on the brass surfaces in the environment. More studies are planned.

This work was supported by the DOE Grant No. DEFG02-96ER45439 through the Materials Research Laboratory at the University of Illinois at Urbana-Champaign.

References

Colling, J.H., Whindcup, P.A.E. & Hayes, C.R. (1987). J. Inst. Water & Envir. Manag., **1**, 263.

Korshin, G.V., Ferguson, J.F. & Perry, S.A.L. (1996). J. American Water Works Association, **88**, No.7, 36.

Ferguson, J.F., van Franqué, O. & Schock, M.R. (1996). Corrosion of Copper in Potable Water Systems. In *Internal Corrosion of Water Distribution Systems*. Denver, Co.

Schock, M.R. (1989). J. American Water Works Association, **81**, No.7, 88.

Schock, M.R., Wagner, L. & Oliphant, R.J. (1996). Corrosion and Solubility of Lead in Drinking Water. In *Internal Corrosion of Water Distribution Systems*. Denver, Co.

Schock, M.R. (1980). J. American Water Works Association, **72**, 695.

Shoesmith, D.W., Bailey, M.G. & Taylor, P. (1988). Can. Journ. Chem., **66**, 2941.

Stern, E. A., Newville, M., Ravel, B., Yacoby, Y. & Haskel, D. (1995). Physica B, **208 & 209**, 117.

Taylor, P. & Lopata,V.J. (1984). Can. Journ. Chem., **62**, 395.

Zabinsky, S. I., Rehr, J. J., Ankudinov, A., Albers, R. C., & Eller, M. J. (1995). Phys. Rev. B, **52**, 2995.

(Received 10 August 1998; accepted 18 November 1998)